at low density (2×10^3 cells/cm^2), and then cultured for 3 days. The numbers of hiPSCs passaged in PBS$^{ca/-}$ were higher than those passaged in PBS$^{-/-}$ (253G1: Fig. 2c, 201B7 & Tic: Supplementary Fig. 4c), suggesting that adding physiological concentration of Ca^{2+} to the dissociation solution increases cell survival rates by decreasing dissociation-induced apoptosis.

It is also known that enzymatic digestion damages hPSCs[5,8]. We first used dispase, an enzyme often used to passage hPSCs under serum- and feeder-free conditions (Table 1)[20]. Because we routinely use 0.025–0.6 U/ml dispase (0.05–300 mg/ml), depending on the enzyme activity and on storage conditions[14], excess dispase (1 U/ml) was used to evaluate its damaging effect with the expectation that dispase dissociation of cell-cell binding would decrease the size of cell clumps, resulting in apoptosis. However, addition of 1 U/ml dispase in PBS$^{-/ca}$ did not decrease hPSC clump size (253G1: Fig. 2d, 201B7: Supplementary Fig. 4d). Indeed, large clumps of annexin V-FITC-negative cells were also found when dispase was added to the PBS$^{ca/-}$ (253G1: Fig. 2e, 201B7: Supplementary Fig. 4e), and quantitative analysis by FCM revealed that the relative percentages of annexin V-FITC-positive apoptotic cells were not changed by addition of dispase (253G1: Fig. 2f, 201B7: Supplementary Fig. 4f). The results were the same when 0.25% trypsin was added to PBS$^{ca/-}$, despite trypsin having more potent protease activity than dispase (Supplementary Fig. 5a–c, e–g). These findings together suggested that adding proteolytic enzyme to the PBS$^{ca/-}$ dose not decrease the cell clump size and thus does not increase dissociation-induced apoptosis. Our results are consistent with a previous report that Ca^{2+} protects against trypsinization of cell-cell binding[10]. Because Ca^{2+} did not affect the cell-fibronectin binding during dissociation (Fig. 1bc, Supplementary Fig 1a), we next measured the re-attachment ability of hiPSCs to fibronectin-coated surfaces. To do this, hPSCs were incubated with dispase in PBS$^{ca/-}$, and replated in ESF9a medium with RI for counting the next day. The reattachment efficiency decreased with increasing concentrations of dispase, and the mean efficiency values at 1 U/ml dispase were smaller than those for PBS$^{ca/-}$ alone (253G1: Fig. 2g, 201B7: Supplementary Fig. 4g); a similar result was attained when trypsin was added to PBS$^{ca/-}$ (Supplementary Fig. 5dh). These results suggested that addition of enzyme damages cells by suppressing cell-fibronectin rebinding rather than by increasing apoptosis.

These results showed that enzyme-free solution containing a physiological concentration of Ca^{2+}, without Mg^{2+}, enables passaging of hPSCs with less cell damage than found using either divalent-free solution or Ca^{2+}-containing solution with enzyme (dispase or trypsin).

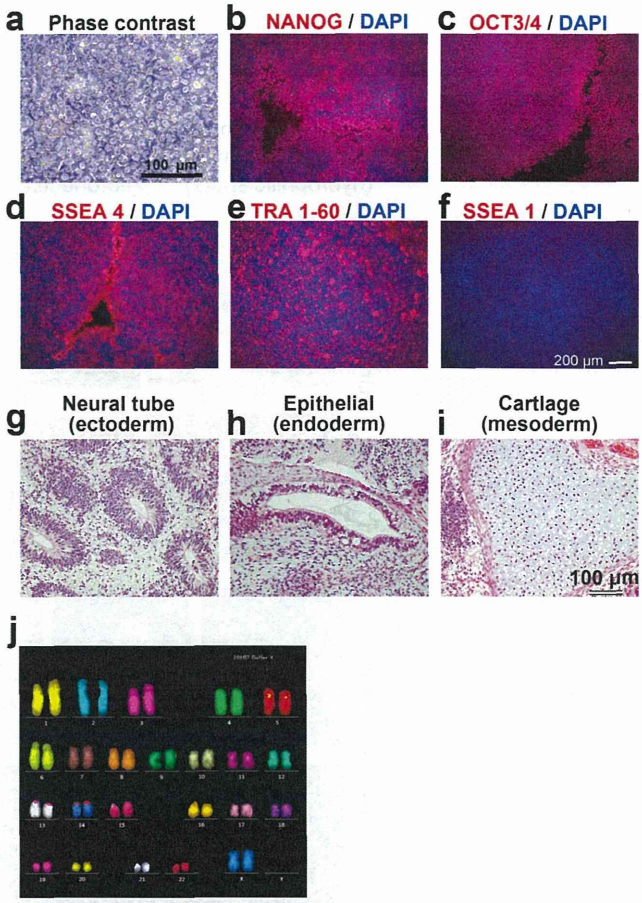

Figure 3 | Passage solution with Ca^{2+} and without Mg^{2+} supports long-term culture and pluripotency of hPSCs. The hiPSC 201B7 were cultured for 15 passages under the ESF-Fb-EzF condition. (a): Phsecontrast micrograph. (b–f): Immunocytochemistry showed that the cells expressed self-renewal markers, NANOG ((b): red), OCT3/4 ((c): red), SSEA4 ((c): red) and TRA 1–60 ((e): red), but not an early differentiation marker, SSEA1 ((f): red). The nuclei were stained with DAPI (blue). (g–h): Histological analysis with HE staining demonstrated that hiPSC-derived teratoma contained derivatives of all three germ layers: neural tube ((g): ectoderm), epitherial ((h): endoderm), and cartridge ((i): mesoderm). (j): FISH karyotype analysis showed a normal karyotype (46XX). Scale bars are 100 μm (a, g–i) or 200 μm (b–f).

Long-term culture of hPSCs with enzyme-free passaging. Next, we tried long-term culturing of hPSCs under enzyme-, serum-, and feeder-free culture conditions. Two hiPSC lines, 253G1 and 201B7, were successfully cultured for more than 10 passages in ESF9a medium on fibronectin-coated dishes by using the solution with Ca^{2+} and without Mg^{2+} (ESF-Fb-EzF condition), with both cell types expressing self-renewal markers (Supplementary Fig. 6a–c, j–l). Immunocytochemistry of embryoid bodies derived from the two cell lines indicated that pluripotency was maintained (Supplementary Fig. 6dm). Unexpectedly, karyotype abnormalities were found not only under the ESF-Fb-EzF condition (Supplementary Fig. 6ir) but also in the sister cultures under the other conditions (Supplementary Fig. 6hopq), suggesting that the abnormalities were induced before enzyme-, serum-, and feeder-free culture.

To confirm the karyotype normality, we newly performed long-term cultures using hiPSC 201B7 and Tic lines. The 201B7 cell line was pre-validated to ensure a normal karyotype, and then cultured under the ESE-Fb-EzF condition for more than 10 passages. The cells formed normal hiPSC colonies, which were tightly packed, and flat colonies consisting of cells with large nuclei and scant cytoplasm (Fig. 3a)[1–3] and expressed four self-renewal markers, NANOG, OCT3/4, SSEA4 and TRA 1–60 but not an early differentiation marker, SSEA1 (Fig. 3b–f). The cells differentiated into derivatives of all three primary germ layers *in vivo* using teratoma formation (Fig. 3g–i). The cells showed a normal karyotype (Fig. 3j). Karyotype after long-term culture was also normal in another hiPSC line, Tic (Supplementary Fig. 7), confirming that karyotype remained stable during the enzyme-, serum-, and feeder-free culture. These results suggested that enzyme-free culture is a useful method for routine culturing of hPSCs.

Cell sheet harvesting. Finally, we tried cell sheet harvesting using our enzyme-free solution. Cell sheet harvesting using special equipment such as a temperature-responsive surface and magnet followed by transplantation is one of the most promising approaches for applying hPSCs to regenerative medicine[21,22]. However, in this study, simple incubation in PBS with Ca^{2+} followed by gentle pipetting enabled us to harvest the cells as 2-mm-diameter sheets without cells splitting off (Fig. 4a–e) and without specialized equipment. Similar results were obtained for early-differentiated cells induced by bone

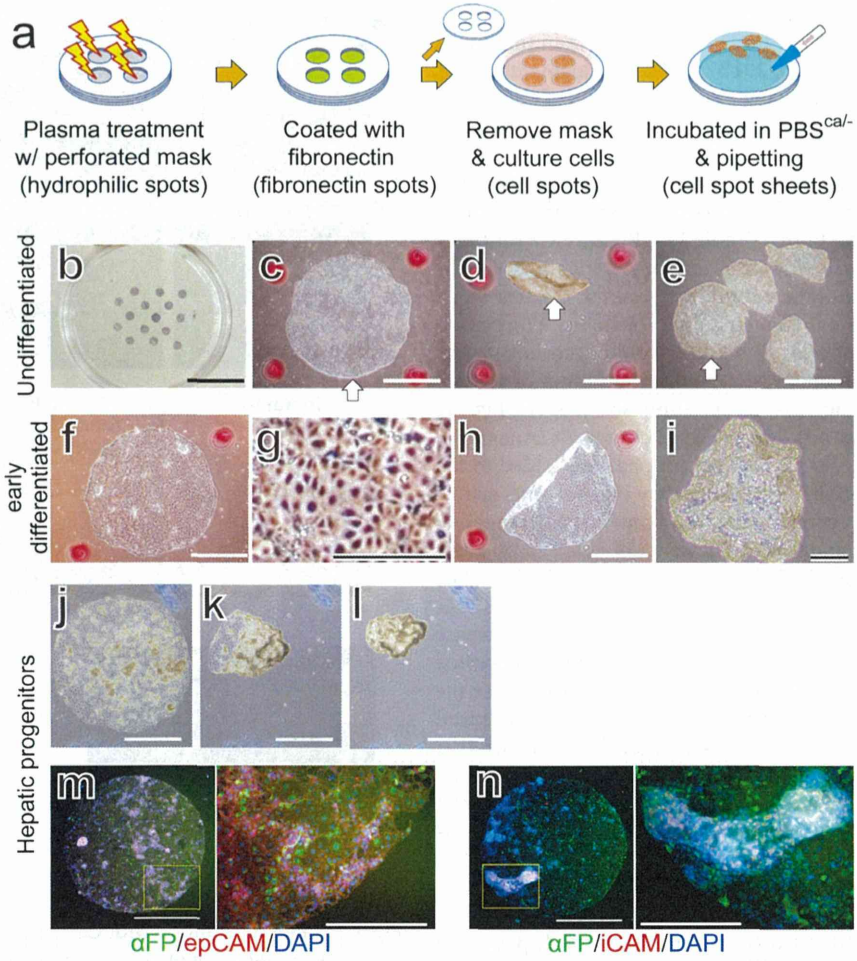

Figure 4 | Cell sheet harvesting. (a): Schematics of spot sheet formation. The hiPSCs (253G1) were cultured in ESF9a medium (undifferentiated: (b–e)), ESF6 medium supplemented with BMP4 for two days (early differentiated: (f–i)). The hiPSC (Tic)-derived hepatic progenitors (j–n). The illustrations were drawn by KO. (b): ALP staining of the hiPSCs plated on 2-mm-diameter fibronectin spots. Phase-contrast micrographs before (c, f, g, j), during (h, k), and after (d, e, i, l) 15 min in $PBS^{ca/-}$ followed by pipetting. (g) is a magnified image of part of (f). The white arrows indicate the same cell spot sheet (c, d, e). The red spots in (c–e, f, h, i) and blue irregular marks in (j–l) are position makers. (mn): Immunohistochemistry of hepatic progenitors using the early stages of liver development marker, α-fetoprotein (αFP: green), EpCAM (red), and iCAM (red). Nuclei were stained with DAPI (blue). The right panels are magnified images of the boxed areas in the left panels. Scale bars are 1 cm (b), 1 mm ((c–f, h, j–l), left of (mn)), and 400 μm ((g, i), right of (m,n)).

morphogenetic protein 4 (BMP4) (Fig. 4f–i) and for hiPSC-derived hepatic progenitors (Fig 4j–n), suggesting that the PBS with Ca^{2+} could be used to routinely and simply harvest cells as a large sheet without special equipment.

Discussion

The present study showed that cell-fibronectin and cell-cell binding are controlled separately by Mg^{2+} and Ca^{2+}, respectively, in hPSC cultures. Using enzyme-free solutions containing Ca^{2+} without Mg^{2+}, we successfully passaged hPSCs cultured under serum- and feeder-free conditions as large cell clumps that showed less damage than those passaged in divalent cation-free solution or with dispase or trypsin. The cells were also harvested as a cell sheet without the need for splitting off.

The cell clumps dissociated by $PBS^{ca/-}$ (1 mM Ca^{2+} and 0 mM Mg^{2+}) and represented in Fig 2d were smaller than those represented in Fig 1e. The decreased cell clump size might be caused by the DNase added in all enzyme-related experiments (Fig 2d–g, and Supplementary Fig 4d–g and 5) to reduce the abundance of free-floating DNA fragments derived from damaged cells. Such addition of DNase might reduce cell-cell attachments arising from the free DNA fragments, and thereby also reduce cell clump size. However, even in the presence of DNase, the cell clumps dissociated by $PBS^{Ca/-}$ without enzyme were significantly larger than those dissociated by $PBS^{-/-}$ without enzyme (Supplementary Fig 5ae).

Addition of enzyme increased the sizes of cell clumps in three of the four conditions in the presence of calcium (Fig 2d, Supplementary Fig 4d and 5ae). A possible reason for this size increase tendency is enzymatic digestion of some cell-fibronectin attachment that enabled cell colonies to detach more easily from the dish. Consequently, large colonies may be harvested intact with less splitting of cell-cell binding by pipetting.

Commonly, hPSCs are passaged with enzyme and in medium containing physiological concentrations of Mg^{2+} and Ca^{2+} (Fig. 5 upper right)[1,2]. Single-cell culture methods such as clonal isolation are achieved by dissociating cells in solutions containing low Mg^{2+} and Ca^{2+} concentrations (Fig. 5 lower left)[4,6,8]. In the present study we showed that hPSC cell-cell binding can be disrupted with less cell detachment from the dish surface in a solution containing high Mg^{2+}, but low Ca^{2+} concentrations (Fig. 5 upper left), and that large cell clumps and sheets can then be harvested by dissociating in low Mg^{2+} and high Ca^{2+} solution (Fig. 5 lower right).

The serum-, feeder-, and enzyme-free composition described herein could provide practical culture methods for controlling

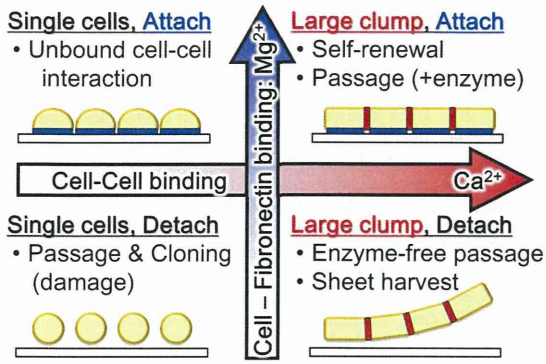

Figure 5 | Schematics of the effects of Mg^{2+} and Ca^{2+} on hPSCs culture.

hiPSCs physical interactions and thus enable further studies into the effects of such interactions and of endogenous and exogenous factors on cells, with the added benefit of eliminating instability caused by lot differences in enzyme. Moreover, such defined culture conditions could facilitate a stable and safe source of hiPSCs for potential clinical applications.

Methods

hPSCs culture. The hESC HUES8[19], H9 (WA09)[1], KhES1, and KhES3[23] lines were obtained from Harvard University (Cambridge, MA, USA), from WiCell Research Institute (Madison, WI, USA), or from Kyoto University (Kyoto, Japan). The hiPSC 201B7[2] and 253G1[18] lines were obtained from RIKEN BRC Cell Bank (Tsukuba, Ibaraki, Japan) through the National Bio-Resource Project for MEXT, Japan and the hiPSCs Tic[24] line (JCRB13331), which was derived from fetal lung fibroblasts (MRC-5), was obtained from JCRB Cell Bank (Osaka, Japan). hPSCs were maintained in a KSR-based medium on mouse embryonic fibroblast (MEF) feeder cells, and subcultured using CTK medium (KSR-MEF-CTK condition), as described in Supplementary Methods. In all experiments, hPSCs maintained in KSR-based medium on MEFs were transferred into serum-free medium, hESF9a on fibronectin-coated dishes, and passaged at least once before assaying (Supplementary Methods). The culture dishes were coated with 2 μg/cm² fibronectin from human plasma (063-05591; Wako) or from bovine plasma (F-1141; Sigma, St. Louis, MO, USA) in PBS for at least 30 min at 37°C, and then excess solution was removed. For subculturing, the cells were detached from the culture dish using 0.2–0.5 U/ml dispase (17105-041; Life Technologies, Grand island, NY, USA) in hESF9a medium and replated in hESF9a medium with 5 μM ROCK inhibitor (RI, Y-27632; Wako). The hESF9a medium (ESF-Fb-Dsp condition) was changed daily.

For long-term culture under enzyme-, serum- and feeder-free condition (ESF-Fb-EzF condition), the cells were passaged with enzyme-free passage solution containing divalent cation-free DMEM-F12 medium (Supplementary table 1) supplemented with the same factors found in ESF9a medium. For subculturing, the cells were rinsed twice with $PBS^{-/-}$ and once with the enzyme-free passage solution, before being incubated in the same solution for more than 15 min at 37°C, and then triturated with a 1-ml micropipette tip. The cells were finally harvested by gentle centrifugation (1 min at 10 G) or stood for a few minutes before replating in hESF9a medium with 5 μM RI. Medium was changed daily.

Embryoid bodies formation. *In vitro* differentiation was induced by the formation of embryoid bodies as described previously[14]. Undifferentiated hiPSCs were cultured by floating in DMEM-F12 medium supplemented with 20% KSR, 0.1 mM 2-mercaptoethanol, and MEM non-essential amino acids (Life Technologies). The floating embryoid bodies were then replated onto 1 mg/ml gelatin-coated dishes in DMEM with 10% FBS. The medium was changed every other day with the same floating culture solution.

Karyotype analysis. Metaphase spreads were prepared from cells treated with colcemid (KaryoMAX Colcemid, Gibco 15212-012, final concentration of 40 ng/ml, overnight treatment) or metaphase arresting solution (Genial Genetic Solutions Ltd., Cheshire, UK). We performed a standard G-banding or multicolour fluorescence in situ hybridization (FISH) karyotypic analysis on at least 20 metaphase spreads for each population. For FISH karyotype analysis, 24XCyte Human Multicolor FISH Probe Kit (MetaSystems GmbH Altlussheim, Germany) were used.

Cell detachment and dissociation assay. The dose response size and removal ratio of hPSCs cultured on divalent cations using 24-well plates were measured as follows. The cells cultured in ESF9a on fibronectin-coated dishes were detached and dissociated into cells clump using 0.2–0.5 U/ml dispase, and then were plated in ESF9a medium on 24-well plates coated with 2 μg/cm² fibronectin (Wako) at 37°C for more than 1 hour. At 4 or 5 days after plating, the attached cells were stained with 1 μM calcein-AM (Dojindo, Kamimashiki, Kumamoto, Japan), a fluorescent living cell dye, for 20 min at 37°C, and imaged as the control state. Then the cells were rinsed once with $PBS^{-/-}$, rinsed again with PBS containing various concentration of Ca^{2+} and Mg^{2+}, incubated in the same PBS for a further 15 min at 37°C, and then triturated 5 times with a 1-ml micropipette tip. For enzymatic digestion experiments, dispase or trypsin was added after 12 min incubation in PBS and left for 3 min. The cells were then triturated 5 times with a 1-ml micropipette tip in the presence of 1 mg/ml DNase I (Roche, Basel, Switzerland), 250 μg/ml trypsin inhibitor (Life Technologies), and 1 mg/ml BSA (sigma), and then 10X volumes of $PBS^{ca/-}$ were added before spinning down the cells. The detached cells were then transferred to another plate, and the remaining cells were imaged for green fluorescence to estimate detachment efficiency. The detached cell clumps were placed between cover slips and cell clump size was estimated based on fluorescent signal using Image J software (NIH, Bethesda, MD, USA). To estimate the cell clump sizes, randomly picked cell clumps for each condition in a test were analyzed with Excel software (Microsoft, Redmond, WA, USA). The cell clump size was converted from area (μm²) into the number of cells by using the area of single cells, which was estimated to be 240 ± 86 μm² (mean ± SD, n = 107) in a separate experiment.

Teratoma formation. Teratomas were generated in severe combined immunodeficient (SCID) mice from 201B7 hiPSCs grown under ESF-Fb-EzF conditions for more than 10 passages. The cells harvested by dispase were resuspended in DMEM supplemented with RI (10 μM). The cells from a confluent single well in a 6-well plate were injected into the thigh muscle of a SCID (C.B-17/lcr-scid/scidJcl) mouse (CLEA Japan, Tokyo, Japan). Nine weeks after injection, tumors were dissected, weighed, and then fixed with 10% formaldehyde Neutral Buffer Solution (Nacalai Tesque, Kyoto, Japan). Paraffin-embedded tissue was sectioned and stained with hematoxylin and eosin (HE). All animal experiments were conducted in accordance with the guidelines for animal experiments of the National Institute of Biomedical Innovation, Osaka, Japan.

Alkaline phosphatase (ALP) staining, immunocytochemistry. The hPSCs were stained with an Alkaline Phosphatase Staining Kit II according to the manual (StemGen, Cambridge, MA, USA). Briefly, the cells were rinsed twice with $PBS^{+/+}$ and fixed with Fix Solution from the kit at room temperature for 4 minutes. The fixed cells were rinsed with PBS containing with 0.05% (v/v) Tween20 and incubated in AP Substrate Solution at room temperature for 20 to 30 minutes. Then the cells were rinsed with $PBS^{+/+}$ and photographed.

Immunocytochemistry was performed as described previously[14,17]. Briefly, hiPSCs were fixed in 4% formaldehyde with 0.5 mM $MgCl_2$ and 0.5 mM $CaCl_2$. Then the cells were permeabilized and blocked with PBS containing 0.1–0.2% Triton X-100, 10 mg/ml BSA, 0.5 mM $MgCl_2$, and 0.5 mM $CaCl_2$, and then reacted with primary antibodies in the solution. The primary antibody binding was visualized using secondary antibodies. Antibody information is listed in Supplementary Table 2. Nuclei were stained with 1 μM DAPI (Wako). Micrographs were taken using a BZ-8100 fluorescence microscope (Keyence, Osaka, Japan).

Flow cytometry (FCM). FCM analysis was performed as described previously[14,17]. All cells were removed from culture dishes using 0.02% (w/v) EDTA-4Na in $PBS^{-/-}$ and then fixed in 4% formaldehyde. The fixed cells were permeabilized and blocked with $PBS^{-/-}$ containing 0.1–0.2% Triton X-100 and 10 mg/ml BSA, and then reacted with primary antibodies in the solution. The primary antibody binding was visualized with secondary antibodies. Antibody information is listed in Supplementary Table 2. A cell sorter (JSAN, Bay Bioscience Co., Ltd., Hogo, Japan) was used for data acquisition.

Apoptosis. An annexin V-FITC apoptosis detection Kit was used to detect cell surface phosphatidylserine (BioVision, Milpitas, CA, USA). Cells were floating cultured for four hours in ESF9a solution following detachment and dissociation. For FCM analysis, the cells were re-dissociated by incubating in 0.02% EDTA solution followed by trituration using a 1-mL pipette tip. The living cells were then stained with FITC conjugate annexin V (1 : 100) and 50 μg/ml propidium iodide in binding buffer. The living cells nuclear were stained with 1 μg/ml Hoechst 33342 (Dojindo, Osaka, Japan).

Spot sheet formation. Silicone rubber masks made of polydimethylsiloxane (PDMS, Sylgard 184, 10 : 1 mix; Dow Corning) were perforated with 2-mm-diameter holes using a hole-punch. The bacterial culture dish (non-cell-attachment-treated dishes, Iwaki) with PDMS masking were treated for 60 seconds by air plasma to make hydrophilic spots (YHS-R, SAKIGAKE-Semiconductor Co., Ltd), then coated with 2 μm/cm² fibronectin for more than 1 hour at 37°C to make fibronectin spots. After rinsing twice with $PBS^{-/-}$, the PDMS mask was removed and the dish was sterilized under a UV lamp. hPSCs (253G1) cultured under the ESF-Fb-Dsp condition or hiPSC Tic-derived hepatic progenitors were dissociated in calcium- and magnesium-free solution, and then plated in ESF9a solution with 5 μg/ml RI or in CDM medium with 50 ng/ml FGF10 with RI.

Early differentiation was induced by 2 days cultivation in the ESF6 medium with 2 ng/ml recombinant human BMP4 (314-BP, R&D Systems, Inc, Minneapolis, MN, USA) as described previously[17]. Hepatic progenitors were differentiated based on the previously reported protocol[25]. Briefly, the hiPSC Tic line was passaged and grown for 2 days in CDM medium[26]. hiPSCs were then grown for 3 days in CDM/PVA medium[26] with 100 ng/ml activin, 20 ng/ml basic FGF, 10 ng/ml BMP4, and 10 μM LY294003 (9901, Cell Signaling Technology, Beverly, MA, USA), followed by 3 days

differentiation in CDM/PVA medium with 50 ng/ml recombinant human FGF10 (345-FG-025/CF, R&D Systems).

Data analysis. Image analyses were performed with Image J software (NIH). Statistical analyses were performed with R software (http://www.r-project.org).

1. Thomson, J. A. *et al.* Embryonic stem cell lines derived from human blastocysts. *Science* **282**, 1145–1147 (1998).
2. Takahashi, K. *et al.* Induction of pluripotent stem cells from adult human fibroblasts by defined factors. *Cell* **131**, 861–872 (2007).
3. Yu, J. *et al.* Induced pluripotent stem cell lines derived from human somatic cells. *Science* **318**, 1917–1920 (2007).
4. Amit, M. *et al.* Clonally derived human embryonic stem cell lines maintain pluripotency and proliferative potential for prolonged periods of culture. *Dev Biol* **227**, 271–278 (2000).
5. Mitalipova, M. M. *et al.* Preserving the genetic integrity of human embryonic stem cells. *Nat Biotechnol* **23**, 19–20 (2005).
6. Watanabe, K. *et al.* A ROCK inhibitor permits survival of dissociated human embryonic stem cells. *Nat Biotechnol* **25**, 681–686 (2007).
7. Ohgushi, M. *et al.* Molecular pathway and cell state responsible for dissociation-induced apoptosis in human pluripotent stem cells. *Cell Stem Cell* **7**, 225–239 (2010).
8. Beers, J. *et al.* Passaging and colony expansion of human pluripotent stem cells by enzyme-free dissociation in chemically defined culture conditions. *Nat Protocols* **7**, 2029–2040 (2012).
9. Shirayoshi, Y., Okada, T. S. & Takeichi, M. The calcium-dependent cell-cell adhesion system regulates inner cell mass formation and cell surface polarization in early mouse development. *Cell* **35**, 631 (1983).
10. Pertz, O. *et al.* A new crystal structure, Ca^{2+} dependence and mutational analysis reveal molecular details of E-cadherin homoassociation. *EMBO J* **18**, 1738–1747 (1999).
11. Mould, A. P., Akiyama, S. K. & Humphries, M. J. Regulation of integrin $\alpha5\beta1$-fibronectin interactions by divalent cations. Evidence for distinct classes of binding sites for Mn^{2+}, Mg^{2+}, and Ca^{2+}. *J Biol Chem* **270**, 26270–26277 (1995).
12. Braam, S. R. *et al.* Recombinant Vitronectin Is a Functionally Defined Substrate That Supports Human Embryonic Stem Cell Self-Renewal via $\alpha V\beta5$ Integrin. *Stem Cells* **26**, 2257–2265 (2008).
13. Rowland, T. J. *et al.* Roles of Integrins in Human Induced Pluripotent Stem Cell Growth on Matrigel and Vitronectin. *Stem Cells Dev* **19**, 1231–1240 (2009).
14. Hayashi, Y. *et al.* Reduction of N-Glycolylneuraminic Acid in Human Induced Pluripotent Stem Cells Generated or Cultured under Feeder- and Serum-Free Defined Conditions. *PLoS ONE* **5**, e14099 (2010).
15. Fadeev, A. G. & Melkoumian, Z. Synthetic Surfaces for Human Embryonic Stem Cell Culture. *Embryonic Stem Cells - Basic Biology to Bioengineering*. Kallos, M. S.(ed.) 89–104 (Intech, rijeka, 2011).
16. Furue, M. K. *et al.* Heparin promotes the growth of human embryonic stem cells in a defined serum-free medium. *Proc Natl Acad Sci U S A* **105**, 13409–13414 (2008).
17. Yoshimitsu, R. Microfluidic Perfusion Culture of Human Induced Pluripotent Stem Cells under Fully Defined Culture Conditions. *Biotechnol Bioeng* (In press).
18. Nakagawa, M. *et al.* Generation of induced pluripotent stem cells without Myc from mouse and human fibroblasts. *Nature Biotechnol* **26**, 101–106 (2007).
19. Cowan, C. A. *et al.* Derivation of embryonic stem-cell lines from human blastocysts. *N Engl J Med* **350**, 1353–1356 (2004).
20. International Stem Cell Initiative Consortium. Comparison of defined culture systems for feeder cell free propagation of human embryonic stem cells. *In Vitro Cell Dev Biol Anim* **46**, 247–258 (2010).
21. Nishida, K. *et al.* Corneal reconstruction with tissue-engineered cell sheets composed of autologous oral mucosal epithelium. *New Eng J Med* **351**, 1187–1196 (2004).
22. Kito, T. *et al.* iPS cell sheets created by a novel magnetite tissue engineering method for reparative angiogenesis. *Sci Rep* **3**, 1418 (2013).
23. Suemori, H. *et al.* Efficient establishment of human embryonic stem cell lines and long-term maintenance with stable karyotype by enzymatic bulk passage. *Biochem Biophys Res Commun* **345**, 926–932 (2006).
24. Nishino, K. *et al.* DNA Methylation Dynamics in Human Induced Pluripotent Stem Cells over Time. *PLoS Genetics* **7**, e1002085 (2011).
25. Touboul, T. *et al.* Generation of functional hepatocytes from human embryonic stem cells under chemically defined conditions that recapitulate liver development. *Hepatology* **51**, 1754–1765 (2010).
26. Vallier, L. *et al.* Signaling Pathways Controlling Pluripotency and Early Cell Fate Decisions of Human Induced Pluripotent Stem Cells. *Stem Cells* **27**, 2655–2666 (2009).
27. Draper, J. S. *et al.* Recurrent gain of chromosomes 17q and 12 in cultured human embryonic stem cells. *Nat Biotechnol* **22**, 53–54 (2004).
28. Ellerström, C., Strehl, R., Noaksson, K., Hyllner, J. & Semb, H. Facilitated Expansion of Human Embryonic Stem Cells by Single-Cell Enzymatic Dissociation. *Stem Cells* **25**, 1690–1696 (2007).
29. Ludwig, T. E. *et al.* Feeder-independent culture of human embryonic stem cells. *Nat Methods* **3**, 637–646 (2006).
30. Klim, J. R., Li, L., Wrighton, P. J., Piekarczyk, M. S. & Kiessling, L. L. A defined glycosaminoglycan-binding substratum for human pluripotent stem cells. *Nat Methods* **7**, 989–994 (2010).

Acknowledgments

The authors would like to thank Reiko Terada at The University of Tokyo for the culturing of hPSCs, and Kumiko Higuchi at AIST for karyotype analysis. This work was supported in part by Grants-in-Aid for Scientific Research and the Project for Realization of Regenerative Medicine from the Ministry of Education, Science, Sports, Culture and Technology (MEXT) of Japan to KO and TM, by Promotion of Independent Research Environment for Young Researchers funding to KO, by an Adaptable & Seamless Technology Transfer Program through Target-driven R&D (A-Step) of the Japan Science and Technology agency (JST) to KO, and by grants from the Ministry of Health, Labour, and Welfare of Japan to KO and MKF. The funding bodies had no role in study design, data collection and analysis, decision to publish, or preparation of the manuscript.

Author contributions

K.O. prepared all figures and supplementary figures. S.T. prepared figure 1, 2 and 4 and supplementary figure 1, 3, 4, 5 and 6. A.F., K.Y. and M.K.F. prepared Figure 3, 4 and Supplementary Figure 7. Y.I., Y.O. and M.A. prepared supplementary figure 6. Y.H., T.C., T.M. and M.A. prepared Supplementary Figure 2. K.O., Y.H. and M.K.F. wrote the manuscript text. All authors reviewed the manuscript.

Additional information

Supplementary information accompanies this paper at http://www.nature.com/scientificreports

Competing financial interests: The authors declare no competing financial interests.

How to cite this article: Ohnuma, K. *et al.* Enzyme-free Passage of Human Pluripotent Stem Cells by Controlling Divalent Cations. *Sci. Rep.* **4**, 4646; DOI:10.1038/srep04646 (2014).

STEM CELLS®

EMBRYONIC STEM CELLS/INDUCED PLURIPOTENT STEM CELLS

Biosynthesis of Ribosomal RNA in Nucleoli Regulates Pluripotency and Differentiation Ability of Pluripotent Stem Cells

KANAKO WATANABE-SUSAKI,[a] HITOMI TAKADA,[a] KEI ENOMOTO,[b] KYOKO MIWATA,[a] HISAKO ISHIMINE,[a] ATSUSHI INTOH,[c] MANAMI OHTAKA,[a] MAHITO NAKANISHI,[a] HIROMU SUGINO,[a] MAKOTO ASASHIMA,[a,c,d,e] AKIRA KURISAKI[a,f]

Key Words. Fibrillarin • Ribosomal RNA • Embryonic stem cells • Pluripotency • Nucleoli • Differentiation

ABSTRACT

Pluripotent stem cells have been shown to have unique nuclear properties, for example, hyperdynamic chromatin and large, condensed nucleoli. However, the contribution of the latter unique nucleolar character to pluripotency has not been well understood. Here, we show that fibrillarin (FBL), a critical methyltransferase for ribosomal RNA (rRNA) processing in nucleoli, is one of the proteins highly expressed in pluripotent embryonic stem (ES) cells. Stable expression of FBL in ES cells prolonged the pluripotent state of mouse ES cells cultured in the absence of leukemia inhibitory factor (LIF). Analyses using deletion mutants and a point mutant revealed that the methyltransferase activity of FBL regulates stem cell pluripotency. Knockdown of this gene led to significant delays in rRNA processing, growth inhibition, and apoptosis in mouse ES cells. Interestingly, both partial knockdown of FBL and treatment with actinomycin D, an inhibitor of rRNA synthesis, induced the expression of differentiation markers in the presence of LIF and promoted stem cell differentiation into neuronal lineages. Moreover, we identified p53 signaling as the regulatory pathway for pluripotency and differentiation of ES cells. These results suggest that proper activity of rRNA production in nucleoli is a novel factor for the regulation of pluripotency and differentiation ability of ES cells. STEM CELLS *2014;32:3099–3111*

[a]Research Center for Stem Cell Engineering, National Institute of Advanced Industrial Science and Technology (AIST), Higashi 1-1-1, Tsukuba, Ibaraki, Japan; [b]Department of Biological Science, Graduate School of Science, The University of Tokyo, Meguro-ku, Tokyo, Japan; [c]Department of Life Sciences (Biology), Graduate School of Arts and Sciences, The University of Tokyo, Komaba, Meguro-ku, Tokyo, Japan; [d]ICORP Organ Regeneration Project, Japan Science and Technology Agency (JST), Komaba, Meguro-ku, Tokyo, Japan; [e]Life Science Center of Tsukuba Advanced Research Alliance (TARA), The University of Tsukuba, Tsukuba, Ibaraki, Japan; [f]Graduate School of Life and Environmental Sciences, The University of Tsukuba, Tsukuba, Ibaraki, Japan

Correspondence: Akira Kurisaki, Ph.D., Research Center for Stem Cell Engineering, National Institute of Advanced Industrial Science and Technology (AIST), Higashi 1-1-1, Tsukuba, Ibaraki 305- 8562, Japan. Telephone: +81-29-861-2569; Fax: +81-29-861-2987; e-mail: akikuri@hotmail.com

Received September 24, 2013; accepted for publication July 23, 2014; first published online in STEM CELLS *EXPRESS* September 3, 2014.

1066-5099/2014/$30.00/0

http://dx.doi.org/10.1002/stem.1825

INTRODUCTION

Embryonic stem (ES) cells can undergo self-renewal while retaining the ability to differentiate into all types of cells in the body. Pluripotency of stem cells is regulated by a specific transcription network composed of core transcription factors such as Oct4, Sox2, and Nanog [1, 2]. On the other hand, ES cells have unique nuclear properties such as hyperdynamic chromatin and an unusual morphology of subnuclear compartments, including large nucleoli [3, 4]. In ES cells, the nucleoli undergo dynamic morphological changes during the differentiation process.

Nucleoli are the sites of ribosome biogenesis, ribosomal DNA transcription, pre-ribosomal RNA (rRNA) processing, and assembly of mature rRNAs with ribosomal proteins [5]. Nucleoli also have several roles in cellular processes, including cell-cycle control, regulation of mitosis, biogenesis of multiple ribonucleoproteins, and cellular stress responses [6]. The nucleolar size varies among cells and is dependent mainly on the activity of the organelle: fully active nucleoli are larger, whereas inactive nucleoli tend to be small and fragmented [7]. The size of nucleoli increases in growing cells in proportion to the amount of rRNA synthesized [8, 9]. Although a correlation between the pluripotency of ES cells and the characteristic morphology of nucleoli has been suggested, the direct contribution of nucleoli to pluripotency and differentiation ability of ES cells has not been explored.

Fibrillarin (FBL) is a specific marker for the dense fibrillar component and indispensable for ribosome biogenesis. FBL functions as a catalytic center of C/D box small nucleolar ribonucleoprotein complexes that catalyze the 2′-*O*-methylation of rRNA [10–12]. In yeast, FBL is essential for cell viability [10, 12]. In mice, loss of the methyltransferase domain of FBL by gene targeting led to embryonic lethality before the blastocyst stage [13]. Previously, we performed proteomic analyses of mouse ES cells and identified FBL as one of the highly expressed proteins in pluripotent mouse ES cells [14].

In this study, we investigated the functions of nucleoli in pluripotent ES cells by modulating this principal nucleolar methyltransferase, FBL.

We show that biosynthesis of rRNA regulates the maintenance and differentiation of ES cells through the p53 signaling pathway.

Materials and Methods

Cell Culture

The mouse ES cell line D3 was purchased from the American Type Culture Collection (ATCC, Manassas, VA, http://www.atcc.org). EBRTcH3, a mouse ES cell line used for knock-in experiments, was a kind gift from Drs. Hitoshi Niwa and Shinji Masui (Riken, Japan). These cells were maintained on feeder layers of mitomycin C-treated mouse embryonic fibroblasts (MEFs) or 0.1% gelatin-coated dishes in ES medium, Dulbecco's modified Eagle's medium (DMEM) (high-glucose; Wako, Osaka, Japan, http://www.wako-chem.co.jp/english) containing 15% heat-inactivated fetal calf serum (FCS, Roche, Mannheim, Germany, http://www.roche-applied-science.com), nonessential amino acids (Sigma-Aldrich, St. Louis, MO, http://www.sigmaaldrich.com), 0.1 mM β-mercaptoethanol (Sigma-Aldrich), 0.1 mg/mL penicillin/streptomycin (Wako), and 1,000 U/mL leukemia inhibitory factor (LIF) (ESGRO; Chemicon, Billerica, MA, http://www.chemicon.com). To prepare RNA and protein samples from pluripotent and differentiated cells, mouse ES cells were cultured for 10 days in the above medium in the presence or absence of LIF, respectively.

Plat-E packaging cells were kindly provided by Dr. Kitamura (University of Tokyo, Japan) [15] and were used to produce retroviruses. Plat-E cells were maintained in DMEM (low-glucose; Wako) containing 10% FCS, 0.1 mg/mL penicillin/streptomycin, 1 μg/mL puromycin (Sigma-Aldrich), and 10 μg/mL blasticidin (Life Technologies, Rockville, MD, http://www.lifetech.com). The human cell lines HeLa and HaCaT and the mouse cell lines C2C12 and KUM9 were maintained in DMEM (low-glucose; Wako) containing 10% FCS and 0.1 mg/mL penicillin/streptomycin (Wako). KUM9 cells were generously provided by Dr. Umezawa (NCCHD, Japan).

Plasmid Construction

Full-length and deletion mutants of FBL expression plasmids were constructed with a polymerase chain reaction (PCR)-amplified DNA fragment using plasmids encoding full-length FBL (pcDNA3.1[+]-FBL) and the deletion mutants (pcDNA3.1[+]-FIB IV for FBL-N and FIB III for FBL-C) [16] as templates. The PCR primer sets were as follows: for full-length FBL, forward, 5′-GGA ATT CGC CAC CAT GGA CTA CAA GGA C-3′ and reverse, 5′-GCT CTC GAG TCA GTT CTT CAC CTT GGG GGG-3′; for the deletion mutants of FBL, forward for both FBL-N and FBL-C, 5′-GGA ATT CGC CAC CAT GGA CTA CAA GGA C-3′ and reverse for FBL-N, 5′-CTC GCG GCC GCT CAT CGG TAC TCA ATT TTG TCA TC-3′, and reverse FBL-C, 5-CTC GCG GCC GCT CAG TTC TTC ACC TTG GGG G-3′. The full-length cDNA were amplified with a high-fidelity PCR enzyme, KOD-Plus (TOYOBO, Osaka, Japan, http://www.toyobo.co.jp/), digested with EcoRI and XhoI, and inserted between the EcoRI and XhoI sites of the pCAG-IP vector [17]. Similarly, the deletion mutant cDNAs were amplified and inserted between EcoRI and NotI sites of the same vector. All constructed pCAG-IP-based expression vectors for the generation of FBL proteins were FLAG-tagged at the N-terminus.

Point mutations in FBL were introduced by PCR-based site-directed mutagenesis using KOD-Plus with the following primers: forward, 5′-CTG CCT CGG GCG CCA CGG TCT CCC ATG TCT CTG ACA TCG TTG-3′ and reverse, 5′-CAA CGA TGT CAG AGA CAT GGG AGA CCG TGG CGC CCG AGG CAG-3′. pCAG-IP full-length FBL was used as template. PCR products were treated with DpnI at 37°C for 1 hour to selectively digest the template plasmid. Competent *Escherichia coli* (DH5α) were transformed with DpnI-digested DNA, and the mutated plasmid was selected in lysogeny broth (LB) supplemented with ampicillin.

Retroviral vectors, pMXs-Oct4, pMXs-Sox2, pMXs-Klf4, and pMXs-cMyc, were obtained from Addgene (Cambridge, MA, http://www.addgene.org). The FBL expression retroviral vector was constructed using a PCR-amplified DNA fragment. The PCR primer set was as follows: forward, 5′-GGA ATT CGC CAC CAT GGA CTA CAA GGA C-3′ and reverse 5′-CTC GCG GCC GCT CAG TTC TTC ACC TTG GGG GG-3′. FBL cDNA was amplified with KOD-Plus, digested with EcoRI and NotI, and inserted between the EcoRI and NotI sites of the pMYs vector [15].

Engineered miRNA expression vectors were constructed using the BLOCK-it Pol II miR RNAi expression vector kit (Life Technologies) by inserting the following sense-loop-antisense DNA sequences into the cloning sites of the pcDNA6.2-GW/EmGFP-miR and pcDNA6.2-GW/miR vectors (Life Technologies). The sequences were as follows: FBL miRNA #1, sense, 5′-TGC TGA AAT CAC AAA GTG TCC TCC ATG TTT TGG CCA CTG ACT GAC ATG GAG GAC TTT GTG ATT T-3′, antisense, 5′-CCT GAA ATC ACA AAG TCC TCC ATG TCA GTC AGT GGC CAA AAC ATG GAG GAC ACT TTG TGA TTT C-3′, and FBL miRNA #2, sense, 5′-TGC TGA TTC TTC CCT GAC TGG TTT CCG TTT TGG CCA CTG ACT GAC GGA AAC CAC AGG GAA GAA T-3′, antisense, 5′-CCT GAT TCT TCC CTG TGG TTT CCG TCA GTC AGT GGC CAA AAC GGA AAC CAG TCA GGG AAG AAT C-3′. As a negative control miRNA expression vector, we used the pcDNA 6.2-GW/EmGFP-miR-neg control plasmid (Life Technologies). The negative control sequence without the 5′ overhang was as follows: 5′- GAA ATG TAC TGC GCG TGG AGA CGT TTT GGC CAC TGA CTG ACG TCT CCA CGC AGT ACA TTT-3′.

For the tetracycline (Tc)-off-regulated miRNA expression, the expression cassettes encoding miRNA were amplified with the pcDNA 6.2-GW/EmGFP-mFBL-miR #1 as the template, digested with XhoI and NotI, and inserted between the XhoI and NotI sites of the pPthC vector [18]. The primer set was as follows: forward, 5′-AAA CTC GAG TAG GCG TGT ACG GTG GGA GGC CTA TAT AAG CAG AGC TCG TTT AGT GAA CCG TCA GAT CGC CTG GAG AAT TCG CCA CCC TGG AGG CTT GCT GAA G-3′, reverse, 5′-TTT GCG GCC GCA CAC ACA AAA AAC CAA CAC ACA GAT GTA ATG AAA ATA AAG ATA TTT TAT TGG GCC ATT TGT TCC ATG TGA-3′. For the negative control, pcDNA6.2-GW/miR-neg was used as the template for PCR with the same primers.

Similarly, for the overexpression of FBL, the expression cassette encoding FLAG-FBL was amplified, digested with XhoI and NotI, and inserted between the XhoI and NotI sites of the pPthC vector.

Tc-off-regulated FBL-miRNA-expressing ES cell lines and Tc-off-regulated FBL-expressing ES cell lines were established according to the method of Masui et al. [18]. An EB3 cell-derived mouse ES cell line, EBRTcH3, which has a Tc-off cassette in the ROSA26 locus, was cotransfected with the above targeting vector, pPthC-FBL-miR or pPthC-FLAG-FBL, and a Cre recombinase-expressing vector, pCAGGS-Cre, using Lipofectamine 2000 (Life

Technologies). The cells were cultured in the presence of 1.5 μg/mL puromycin (Sigma-Aldrich) and 1 μg/mL Tc. The established ES clones were cultured in ES medium in the presence or absence of Tc, and the expression of the exogenous gene was examined by immunoblotting and immunofluorescence assay.

For the construction of miRNA-insensitive FBL expression vectors, mutations were introduced into the pCAG-IP-FBL expression vector by PCR-based site-directed mutagenesis using KOD-Plus with the following primers: forward, 5′-CCT GCG TAA TGG TGG ACA TTT CGT AAT ATC CAT TAA GGC CAA CTG-3′ and reverse, 5′-CAG TTG GCC TTA ATG GAT ATT ACG AAA TGT CCA CCA TTA CGC AGG-3′. PCR products were treated with DpnI at 37°C for 1 hour to digest selectively the template plasmid, as described above.

Alkaline Phosphatase Staining

Mouse ES cells were cultured for 10 days in the presence or absence of LIF, fixed with 3.7% formaldehyde in phosphate-buffered saline (PBS) for 5 minutes at room temperature, and then incubated with an alkaline phosphatase substrate, nitro-blue tetrazolium chloride/5-bromo-4-chloro-3′-indoly-phosphate (NBT/BCIP) (Roche), at room temperature to visualize the enzyme activity.

Western Blotting

Cells were lysed in lysis buffer (20 mM Tris-HCl [pH 7.4], 150 mM NaCl, 1 mM EDTA, 1% Nonidet P-40, 1 mM Na_3VO_4, 25 mM NaF, and 25 mM β-glycerophosphate), supplemented with a protein inhibitor cocktail (Complete, Roche), and rotated at 4°C for 1 hour. After centrifugation at 17,000*g* for 10 minutes at 4°C, the supernatants were collected and protein concentrations were determined with a protein assay kit (Bio-Rad, Hercules, CA, http://www.bio-rad.com). Then, 10 μg protein of the whole cell lysate samples was resolved by sodium dodecyl sulfate-polyacrylamide gel electrophoresis and transferred to polyvinylidene fluoride membranes. The membranes were blocked with 5% non-fat skim milk in TBS/Tween-20 (10 mM Tris-HCl [pH 7.4], 150 mM NaCl, 0.1% Tween-20) and incubated with primary antibody overnight at 4°C. After incubation with a horseradish peroxidase-conjugated secondary antibody, the blots were incubated with an enhanced chemiluminescent assay reagent (SuperSignal West Femto, Pierce) for 5 minutes at room temperature, and the protein bands were visualized using an LAS 3000 mini Image Analyzer (Fuji Film). For the quantitative analysis, the protein bands were further analyzed using the Image Gauge software (Fuji Film).

Immunofluorescence Staining

Mouse ES cells were washed with PBS, fixed in 3.7% formaldehyde in PBS for 30 minutes at room temperature, and then permeabilized with 0.5% Triton X-100 in PBS for 5 minutes at room temperature. The cells were blocked with 5% FCS in PBS for 1 hour at room temperature and then incubated with primary antibodies. After washing three times with 5% FCS in PBS for 10 minutes, the cells were incubated with fluorescently labeled secondary antibodies for 1 hour at room temperature, and cell nuclei were stained with 4′,6-diamidino-2-phenylindole (Vector Laboratories, Burlingame, CA, http://www.vectorlabs.com). The cells were observed under a fluorescence microscope (Olympus, IX70) equipped with a CoolSNAP HQ^2 (Photometrics) and processed using MetaMorph software (Molecular Devices, Union City, CA, http://www.moleculardevices.com). A confocal fluorescence microscope (Olympus, FV1000) was also used to analyze the cells.

Immunoprecipitation

Tc-off-regulated FBL-miRNA-expressing ES cells were cultured with or without Tc for 2 days and subsequently harvested for immunoprecipitation. After preparation of whole cell lysates (1 mg of protein) with the lysis buffer as described above, endogenous Mdm2 was immunoprecipitated with 5 μg of antibody against Mdm2 (Santa Cruz Biotechnology Inc., Santa Cruz, CA, http://www.scbt.com, sc-965) and Dynabeads protein G (Life Technologies, 1004D). The immunoprecipitated proteins were detected by immunoblotting with an antibody against L11 (Santa Cruz, sc-25931). An antibody against α-tubulin (Sigma-Aldrich, T9026, 1:3,000) was used as loading control.

Statistical Analysis

Values are expressed as the average ± SEs. The unpaired Student's *t* test was used for comparisons of the parameters between two groups. *p* values less than .05 were considered statistically significant.

Results

FBL is Highly Expressed in ES Cells and Promotes Pluripotency

Our previous differential proteomic analysis identified FBL, a critical methyltransferase indispensable for rRNA processing, as one of the highly expressed nucleolar proteins in pluripotent ES cells [14]. When mouse ES cells were cultured without LIF for 10 days, they differentiated into alkaline phosphatase-negative and morphologically flat cells (Fig. 1A). Under these conditions, the amount of FBL transcript and protein were significantly decreased, that is, to about one-third of that found in pluripotent ES cells, as was observed in pluripotency-specific transcription factors, Nanog and Oct4 (Fig. 1B–1D). Immunofluorescence analysis further confirmed a decrease in FBL in those cells (Fig. 1E). Interestingly, FBL was localized in one or two large condensed foci in the nuclei in pluripotent ES cells. In contrast, in the differentiated cells and non ES cells FBL was detected in multiple scattered small foci in the nuclei (Fig. 1F). A similar morphological change in the nucleoli between pluripotent and differentiated cells has been observed in human ES cells [4]. These results suggested the existence of specific nucleolar functions in pluripotent stem cells.

To explore the functions of nucleoli in ES cells, mouse ES cells stably expressing Flag-tagged FBL were established. These cells showed prolonged alkaline phosphatase activities when cultured without LIF (Fig. 2A). FBL-expressing cells showed sustained expression of Oct4, Nanog, and SSEA-1 even when the cells were cultured for 10 days without LIF (Fig. 2B, 2C). Furthermore, the morphology of the nucleoli was maintained as large foci in FBL-stably expressing cells (Supporting Information Fig. S1). These results suggest that nucleolar FBL has the ability to prolong the pluripotent state of mouse ES cells.

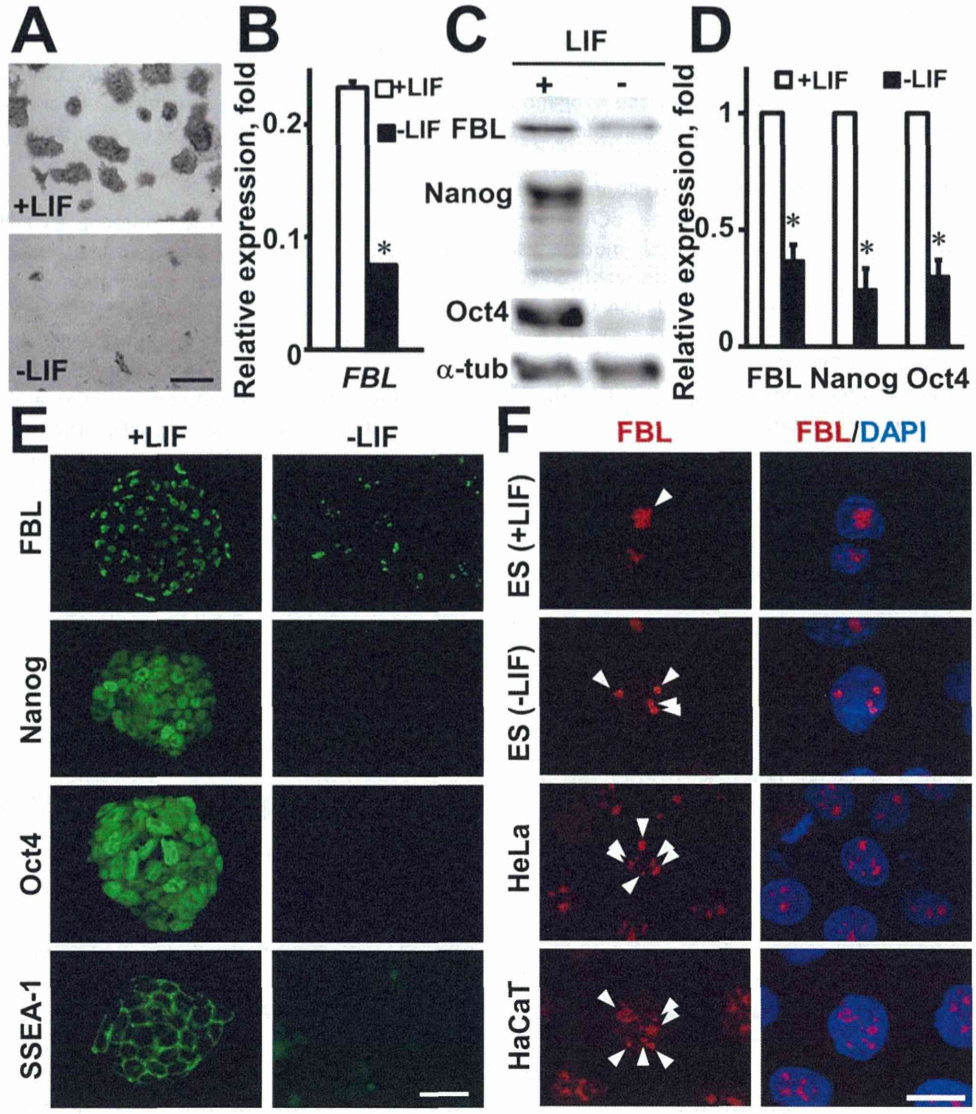

Figure 1. FBL is highly expressed in pluripotent ES cells. Mouse ES cells were cultured for 10 days in the presence (+LIF) or absence of LIF (−LIF) and analyzed for pluripotency marker protein expression. **(A):** Alkaline phosphatase staining. ES cells cultured in the presence of LIF formed tightly packed colonies and had high alkaline phosphatase activity (upper panel), whereas ES cells cultured in the absence of LIF for 10 days showed flattened morphology and lower alkaline phosphatase activity (lower panel). **(B):** Quantitative reverse transcription polymerase chain reaction (qRT-PCR) analysis of *FBL* mRNA. The ES cells were cultured as in (A) for 10 days. **(C):** Western blot analysis of FBL, Nanog, and Oct4 expression. **(D):** Relative densitometric values of the bands. Values were normalized to α-tubulin. Expression levels of FBL, Nanog, and Oct4 in (C) cultured without LIF for 10 days were approximately 36%, 24%, and 30% of that of the cells cultured with LIF, respectively. **(E):** Immunofluorescence staining of FBL, Nanog, Oct4, and SSEA-1. The ES cells were cultured as in (A) for 10 days. **(F):** Localization of FBL in pluripotent and differentiated cells. Arrowheads indicate immunoreactivity of FBL in the nucleus. *, $p < .01$ in (B, D). Scale bars = 300 μm (A), 30 μm (E), and, 20 μm (F). Abbreviations: DAPI, 4′,6-diamidino-2-phenylindole; ES cell, embryonic stem cell; FBL, fibrillarin; LIF, leukemia inhibitory factor.

In contrast, we did not see a clear effect of exogenous FBL expression on pluripotent ES cells cultured with LIF, such as the morphology of ES cells (Fig. 2A), the size of nucleoli (Supporting Information Fig. S1), and the expression of *Nanog* and *Oct4* (Fig. 2B; Supporting Information Fig. S2). One possible explanation for this apparent lack of an effect is that the overexpression of FBL on top of the high levels of endogenous FBL in pluripotent stem cells might not produce an effect as robust as the one observed in the differentiating cells.

Next, we examined the effect of FBL on the reprogramming of somatic cells into induced pluripotent stem (iPS) cells [19]. MEFs were infected with retroviruses that express Oct4, Sox2, Klf4, and c-Myc with or without FBL. Introduction of FBL increased the number of alkaline phosphatase activity-positive colonies as well as the size of the colonies with the transcription factors Oct4, Sox2, and Klf4 (Fig. 2D, 2E), suggesting that nucleolar FBL also regulates the reprogramming process of fibroblasts to pluripotent stem cells. However, this effect was not observed with four factors including c-Myc (Fig. 2E). *FBL* is one of the downstream target genes of c-Myc [20]. Although overexpression of c-Myc induced *FBL* in MEFs, overexpression of FBL failed to induce *c-Myc* (Supporting Information Fig. S3C, S3D). These results suggest that MEFs overexpressing c-Myc already expressed higher levels of

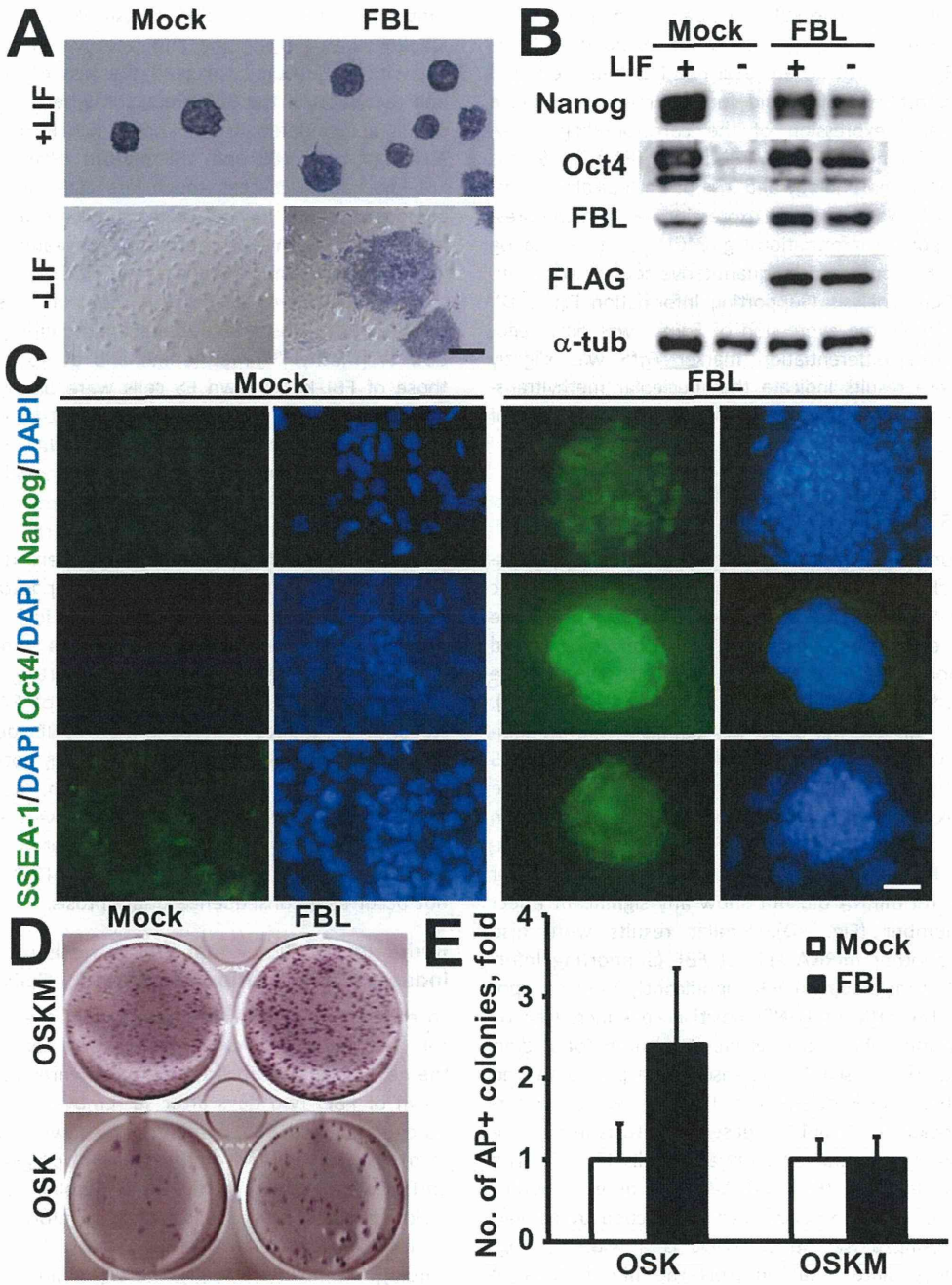

Figure 2. Stable expression of FBL prolongs the pluripotency of embryonic stem (ES) cells in the absence of LIF. ES cells stably expressing FBL or the control vector were cultured for 10 days in the presence or absence of LIF, and the expression levels of pluripotency-specific markers were analyzed. **(A):** Alkaline phosphatase staining of ES cells stably expressing FBL. **(B):** Western blot analysis of Nanog, Oct4, FBL, and FLAG antibodies. **(C):** Immunofluorescence analysis of ES cells with Nanog, Oct4, and SSEA-1 antibodies after culturing without LIF for 10 days. **(D, E):** FBL enhances reprogramming efficiency of mouse embryonic fibroblasts. (D): Alkaline phosphatase staining of induced pluripotent stem (iPS) cells induced with retroviruses for four transcription factors (Oct4, Sox2, Klf4, and cMyc) or three transcription factors (Oct4, Sox2, and Klf4) with or without FBL expression virus. Empty vector pMYs virus was used as control. (E): The colony numbers of iPS cells were counted and normalized to that of the control. Induction of iPS cells was assayed three times independently. Scale bars = 200 μm (A) and 30 μm (C). Abbreviations: AP, alkaline phosphatase; DAPI, 4′,6-diamidino-2-phenylindole; FBL, fibrillarin; LIF, leukemia inhibitory factor; OSK, Oct4, Sox2, and Klf4; OSKM, Oct4, Sox2, Klf4, and cMyc.

endogenous FBL and thus appeared to fail to further promote reprogramming by exogenous FBL.

FBL protein contains a glycine- and arginine-rich (GAR) domain at the N-terminus (Supporting Information Fig. S4A). The C-terminal half, containing a central RNA-binding domain (RBD) and α-helical domain, functions as a methyltransferase; it is highly conserved among many FBL orthologs, from archaebacteria to mammals [11]. The N-terminal GAR-domain is only present in eukaryotes [11, 21]. To locate the functional domain of FBL associated with the maintenance of pluripotency, we established mouse ES cells stably expressing Flag-tagged deletion mutants of FBL (FBL-N and FBL-C, Supporting Information Fig.

S4A). Only ES cells expressing FBL-C showed prolonged alkaline phosphatase activities in the absence of LIF (Supporting Information Fig. S4B). Thr-70 of an archaeal FBL has been reported to be an indispensable amino acid for the methyltransferase activity [22]. Stable expression of the corresponding T-to-A mutation at Thr-172 in the human FBL (T172A FBL) in ES cells resulted in flattened morphology and loss of both alkaline phosphatase activity and Nanog protein expression, even in the presence of LIF (Supporting Information Fig. S4C). Decreased Nanog expression was also confirmed by quantitative reverse transcription PCR (qRT-PCR) analysis (Supporting Information Fig. S4D). In addition to *Nanog*, the expression of *Eomes* was downregulated, whereas the differentiation marker *Fgf5* was slightly upregulated. These results indicate that nucleolar methyltransferase activity is important for the regulation of pluripotency of ES cells.

Nucleolar FBL is Indispensable for the Survival of Pluripotent ES Cells

To verify the functional importance of nucleolar methyltransferase in ES cells, mouse ES cells that express FBL-specific engineered miRNA under the control of the Tc-off inducible promoter were established by using a Cre recombinase-based knock-in method [18]. Removal of Tc from the culture medium induced knockdown of FBL in ES cells (Fig. 3A, 3B). Until 48 hours after removal of Tc, no significant morphological change in FBL-knockdown cells was observed when ES cells were cultured in the presence of LIF. However, the growth of FBL-knockdown ES cells was clearly decreased on day 3. Within 7 days, most of the knockdown ES cells had disappeared (Fig. 3C, 3D). These observations were specific for FBL, as the control miRNA did not show any significant effect on the cell number (Fig. 3D). Similar results were also observed with another miRNA against FBL (Supporting Information Fig. S5). Knockdown of FBL significantly induced apoptosis (Fig. 3E). The ratio of TUNEL-positive cells increased by more than eightfold when ES cells were cultured for 2 days without Tc (Fig. 3F). A sixfold increase of caspase-activated cells was detected after knockdown of FBL (Fig. 3G, 3H). Interestingly, the knockdown of FBL increased apoptosis in pluripotent ES cells but not in the differentiated cells (Fig. 3I) and other non-stem cell lines (Fig. 3H). We also asked whether the phenotypes of FBL knockdown can be rescued by activating rRNA processing/biosynthesis. c-Myc is a widely recognized upstream regulator that controls the biosynthesis of rRNA by inducing RNA polymerase I [23–25], and it promotes the expression of FBL [20]. However, overexpression of c-Myc failed to inhibit FBL-knockdown-induced apoptosis (Supporting Information Fig. S3E, S3F). Only the ectopic expression of the miRNA-insensitive form of FBL rescued ES cells from apoptosis (Supporting Information Fig. S6). These results suggest that highly expressed nucleolar FBL is an indispensable terminal rate-limiting enzyme in rRNA processing and in the survival of pluripotent ES cells.

Nucleolar FBL is a Principal Regulator of rRNA Biosynthesis in Pluripotent ES Cells

Nop1, an ortholog of FBL in yeast, is essential for pre-rRNA processing, and mutations in Nop1 lead to a reduced production rate of mature rRNAs and accumulation of unspliced precursor molecules [10, 12]. Thus, we examined the ribosomal synthesis in FBL-knockdown mouse ES cells using pulse-chase labeling with [^{3}H]-uridine and [methyl-^{3}H]-methionine. Labeling with [^{3}H]-uridine revealed the loss of the 41S precursor and reduction of the 36S precursor, whereas the 34S/32S precursor accumulated in FBL-knockdown ES cells (Fig. 4A, 4B). Although both 28S and 18S mature rRNA were reduced in FBL-knockdown ES cells, much less 18S rRNA was synthesized compared to 28S mature rRNA. A pulse chase labeling experiment with [methyl-^{3}H]-methionine revealed an overall delay in rRNA processing and decreased methylation levels of rRNA in FBL-knockdown ES cells. In control cells, 18S and 28S mature rRNA was first detected immediately after the addition of [methyl-^{3}H]-methionine and at 15 minutes, whereas those of FBL-knockdown ES cells were barely detected at 30 minutes or 45 minutes (Fig. 4C). In FBL-knockdown ES cells, the amount of methionine-labeled rRNA was decreased to 35% of that in control cells (Fig. 4D). Although FBL is the catalytic center of the methyl-transferase complex for rRNA and is essential for the processing of rRNA, there is a possibility that the altered pre-rRNA processing we observed could be one of the indirect outcomes of the complex apoptosis pathway and not a direct consequence of FBL knockdown. To exclude this possibility, we examined the effect of an apoptosis inhibitor on the processing of pre-rRNA (Supporting Information Fig. S7A). At 48 hours after the induction of FBL knockdown, a statistically significant induction of TUNEL-positive cells was detected. Z-VAD-FMK, a caspase inhibitor, potently suppressed the apoptosis induced by FBL knockdown. However, significant amounts of an intermediate 45S rRNA were still accumulated after treatment with Z-VAD-FMK (Supporting Information Fig. S7B), which suggests that altered pre-rRNA processing does not occur as a consequence of apoptosis.

Reduction of Ribosomal Biosynthesis in Nucleoli Induces the Activation of p53 in ES Cells

To examine systematically the effect of the loss of FBL on ES cells, we performed a DNA microarray analysis to screen for the genes that are upregulated or downregulated upon knockdown of FBL. Two days after Tc removal, 1,132 entities were upregulated and 885 entities were downregulated compared to the control cells (twofold change). Upregulated genes were enriched for developmental gene ontology terms in the biological process category (Supporting Information Fig. S8). In contrast, downregulated genes displayed no significant gene ontology term. Interestingly, the expression of other nucleolar proteins, such as nucleostemin, nucleophosmin, and nucleolin was not changed after FBL-knockdown (data not shown), suggesting that the effects of FBL-knockdown are not the indirect effects caused by the other nucleolar regulators. Bioinformatic pathway analysis identified p53 signaling ($p = 2.83E-05$) as the most probable pathway specifically activated in FBL-knockdown ES cells (Fig. 5A). The activity of p53 is regulated by post-translational modification. Phosphorylation of p53 at Ser18 is correlated with the induction of cell-cycle arrest/apoptosis [26], and phosphorylation at Ser389 is observed upon UV irradiation [27, 28] or during the differentiation initiated by nitric oxide (NO) [29] and retinoic acid (RA) [27]. Immunofluorescence and immunoblotting analysis confirmed the induction of p53 expression and its activated form (phosphorylated at Ser18 and at Ser389) after knockdown of FBL in ES cells (Fig. 5B, 5C). The activation of p53 could be induced

